



Effect of radiative source term on the behavior of nanomaterial with considering Lorentz forces

Tran Dinh Manh¹ · Nguyen Dang Nam¹ · Gihad Keyany Abdulrahman² · Ahmad Shafee³ · M. Shamlooei⁴ · Houman Babazadeh^{5,6} · Abdul Khader Jilani⁷ · I. Tiili⁸

Received: 6 July 2019 / Accepted: 17 November 2019 / Published online: 26 November 2019
© Akadémiai Kiadó, Budapest, Hungary 2019

Abstract

An in-house FORTRAN code was developed to analyze the hybrid powders migration within a porous domain which was in appearance of Lorentz force. The permeable 2D enclosure was full of nanomaterial, and properties were selected via empirical formulas. Results indicate that positive impact on Nu_{ave} can be obtained with rise of permeability which is related to greater temperature gradient. Also, similar impact exists for buoyancy force which shows the greater convective flow with rise of Ra. Reduction in temperature gradient with rise of Ha makes the convective flow to reduce.

Keywords Nanomaterial · Radiation · Darcy · Fortran · Lorentz forces

Introduction

In porous media, investigating heat transfer and fluid stream attracted researchers' attentions within the past ten years. Increasing emphasis on fibrous and efficient granular

insulation systems stimulated different investigations in fluid flowing in porous media leading many results to achieve for convective stream in basic geometries in internal and external streams [1–9]. These days, thermal transmission can be improved by applying nanofluids which are typical fluids including nanoparticles [10–25]. In various technologies, natural convection plays the main role in different applications of engineering including—building applications, solar applications and electronic applications. Some problems for industrial ovens or boilers are porous media and nonlinear boundaries of closed or open geometries. In addition, operant fluid might be nanofluids or viscous fluids. Recently, many researchers conducted various studies in nanofluids' convective heat transfer. Typical heat transfer fluids including—oil, ethylene glycol and water—have small rate of k which is a basic restriction in improving the compactness and the efficiency of various electronic applications. Thus, it is required to enhance advanced heat transfer fluids with greater rate of thermal conductivity. By defining nanofluids, such need was tackled [26–40]. Keblinski et al. [41] surveyed possible systems for nanoparticle clustering.

Javed and Siddiqui [42] numerically surveyed the effect of magnetic area on free convection stimulated with ferrofluid which has an inner obstacle. They illustrated that such area leads the strength of flow to weaken. The thermal performance of centered sheet on micropolar liquid flow within a tank was surveyed by Muthtamilselvan et al. [43] who illustrated that the presence of micropolar fluid leads the rate

✉ Houman Babazadeh
houman.babazadeh@tdtu.edu.vn

¹ Institute of Research and Development, Duy Tan University, Da Nang 550000, Viet Nam

² Department of Petroleum Engineering, College of Engineering, Knowledge University, Arbil, Iraq

³ College of Technological Studies, Applied Science Department, Public Authority of Applied Education and Training, Shuwaikh, Kuwait

⁴ Department of Mechanical Engineering, Babol Noshirvani University of Technology, Babol, Islamic Republic of Iran

⁵ Department for Management of Science and Technology Development, Ton Duc Thang University, Ho Chi Minh City, Vietnam

⁶ Faculty of Environment and Labour Safety, Ton Duc Thang University, Ho Chi Minh City, Vietnam

⁷ Department of Computer Science, College of Computer and Information Sciences, Majmaah University, Al-Majmaah 11952, Saudi Arabia

⁸ Department of Mechanical and Industrial Engineering, College of Engineering, Majmaah University, Al-Majmaah 11952, Saudi Arabia

of heat transfer to decrease while increasing non-uniformity terms of sheet outputs in an augment in heat transfer rate.

Societies provided various new ways to reach more capable thermal system [44–72]. Saravanan and Sivaraj [73] numerically studied surface radiation and free convection through an enclosure including adiabatic horizontal walls and vertical cold borders. They applied an in-house code improved on the base of FVM. Based on their results, variable heating raises the ∇T . The mixed convection of viscous fluid flowing inside a tank in appearance of cold vertical borders and inner isothermal triangular heater has been investigated by Gangawane et al. [74] via Fluent software. They found that thermal transition in such system can be improved by applying great Pr number fluids and greater blockage. The impacts of Lorentz on alumina nanomaterial combined behavior within a lid-driven tank including a centrally isothermal body were investigated by Mehmood et al. [75] who found that an increase in Hartmann number reduces the mean Nu, the mean entropy generation and Bejan amount because of heat transfer.

As Eastmen et al. [76] reported that nanomaterials have a considerably greater thermal conductivity rate compared with that of typical ones. The represented stream inside a permeable media has been investigated by Zhang and Liu [77] who applied a numerical technique according to the Brinkman–Forchheimer model. In addition to these, some investigations including LTNE model in a porous media have been conducted. Kalidasan et al. [78] scrutinized the free convection of H_2O -copper nanomaterial in a tank including 2 blocks. They numerically resolved the equations. Based on their results, the mixture effect of unsteady temperature of wall and nanoparticles destroys the hydrodynamic blockage. Free convection of silver powder including centrally hot sheet in the case of cold vertical surfaces was investigated

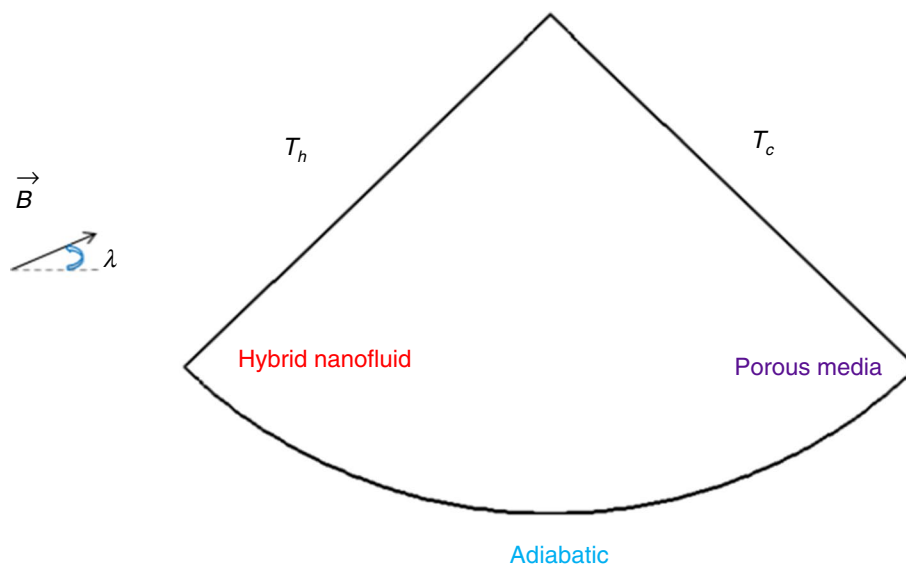
by Mahalakshmi et al. [79] who applied homogeneous model. According to their results, the thermal transmission increases when the concentration of nanoparticle and Re grows. Numerical approaches were developed for complex physics [80–124]. Numerically, free convection within a permeable tilted tank including a centrally solid obstacle under the impact of magnetic area has been studied by Sivaraj and Sheremet [125] who found that an increase in Hartmann amount suppresses the boundary-induced fluid movement and the strength of thermal transition within the enclosure. The empirical results illustrate a much greater thermal conductivity rate compared with that projected by these models. Yu and Choi [126] represented an alternation statement for estimating the thermal conductivity rate of liquid–solid combination. They reported that a structural model of nanofluids may include a bulk liquid and solid nanoparticle.

In current article, a 2D CVFEM simulation was proposed to investigate the impact of Hartmann number on transportation of hybrid nano-powders. To involve the porous media, non-Darcy terms were included in momentum equations and impact of the presence of radiation term was analyzed.

Definition

A curved cavity with three walls was scrutinized (Fig. 1). The left surface is hot, and curved wall is adiabatic. To change the flow pattern, magnetic field has been applied, but we neglected the joule heating because the strength of B is not enough to produce such effect. In current simulation, nanomaterial with hybrid particles as introduced in [127] was selected and properties were calculated based of empirical formulas [127]. To reach the accurate data, in current article, the CVFEM which belongs to Sheikholeslami

Fig. 1 Curved domain with B



[128] was utilized. Regard to its advantages, accurate solution can be obtained. All walls are impermeable. By adding buoyancy effect, the below formulation can be considered:

$$\frac{\partial u}{\partial x} + \frac{\partial v}{\partial y} = 0 \tag{1}$$

$$\begin{aligned} & \frac{\mu_{nf}}{\rho_{nf}} \left(\frac{\partial^2 u}{\partial x^2} + \frac{\partial^2 u}{\partial y^2} \right) + \nu \sigma_{nf} (\cos \lambda) B_0^2 (\sin \lambda) \\ & - \frac{1}{\rho_{nf}} \frac{\partial P}{\partial x} - \frac{\mu_{nf}}{K} u \frac{1}{\rho_{nf}} - (T_c - T) \beta_{nf} g \sin \gamma \\ & + \sigma_{nf} B_0^2 [-u(\sin \lambda)^2] = \nu \frac{\partial u}{\partial y} + u \frac{\partial u}{\partial x} \end{aligned} \tag{2}$$

$$\begin{aligned} & B_0^2 u (\sin \lambda) \sigma_{nf} (\cos \lambda) + \frac{\mu_{nf}}{\rho_{nf}} \left(\frac{\partial^2 v}{\partial x^2} + \frac{\partial^2 v}{\partial y^2} \right) \\ & - g \cos \gamma (T_c - T) \beta_{nf} - \frac{\partial P}{\partial y} \frac{1}{\rho_{nf}} - \frac{1}{\rho_{nf}} \frac{\mu_{nf}}{K} v \\ & + \sigma_{nf} [-v(\cos \lambda)^2] B_0^2 = \nu \frac{\partial v}{\partial y} + u \frac{\partial v}{\partial x} \end{aligned} \tag{3}$$

$$\begin{aligned} & \frac{1}{(\rho C_p)_{nf}} \frac{\partial q_r}{\partial y} + \left(u \frac{\partial T}{\partial x} + v \frac{\partial T}{\partial y} \right) \\ & = k_{nf} (\rho C_p)_{nf}^{-1} \left(\frac{\partial^2 T}{\partial y^2} + \frac{\partial^2 T}{\partial x^2} \right), \tag{4} \\ & \left[T^4 \cong 4T_c^3 T - 3T_c^4, q_r = -\frac{4\sigma_c}{3\beta_R} \frac{\partial T^4}{\partial y} \right] \end{aligned}$$

Regard to previous article [127], we selected hybrid ferrofluid (MWCNT-Fe₃O₄) with base fluid of water. To gain the properties, empirical formulas were applied which are valid for $\phi = 0.003$. Equation (6) was considered to simplify formulas.

$$\psi_y = u, \omega + \frac{\partial u}{\partial y} - \frac{\partial v}{\partial x} = 0, \psi_x = -v, \tag{5}$$

Then, the following equation was developed for the dimensionless variables:

$$\begin{aligned} U &= \frac{uL}{\alpha_{nf}}, (X, Y) = \frac{(x, y)}{L}, \Delta T = \frac{q''L}{k_f}, \\ \Psi &= \frac{\psi}{\alpha_{nf}}, \Omega = \frac{\omega L^2}{\alpha_{nf}}, V = \frac{vL}{\alpha_{nf}} \\ \theta &= \frac{T - T_c}{\Delta T}, \end{aligned} \tag{6}$$

Considering the above equations, Eqs. (8–10) were obtained:

$$\frac{\partial^2 \Psi}{\partial X^2} + \frac{\partial^2 \Psi}{\partial Y^2} = -\Omega, \tag{7}$$

$$\begin{aligned} U \frac{\partial \Omega}{\partial X} + \frac{\partial \Omega}{\partial Y} V &= \frac{A_2}{A_4} \left(\frac{\partial^2 \Omega}{\partial Y^2} + \frac{\partial^2 \Omega}{\partial X^2} \right) \text{Pr} \frac{A_5}{A_1} \\ &+ \text{Pr} \frac{A_6}{A_1} \left(\frac{\partial U}{\partial X} \cos \lambda \sin \lambda - \frac{\partial V}{\partial X} (\cos \lambda)^2 \right. \\ &+ \left. \frac{\partial U}{\partial Y} (\sin \lambda)^2 - \frac{\partial V}{\partial Y} \cos \lambda \sin \lambda \right) \frac{A_2}{A_4} \text{Ha}^2 \end{aligned} \tag{8}$$

$$\begin{aligned} &+ \text{Ra Pr} \left(-\frac{\partial \theta}{\partial Y} \sin \gamma + \frac{\partial \theta}{\partial X} \cos \gamma \right) \\ &\times \frac{A_3 A_2^2}{A_1 A_4^2} - \frac{\text{Pr} A_5 A_2}{\text{Da} A_1 A_4} \Omega, \\ &\left(1 + \frac{4}{3} \left(\frac{k_{nf}}{k_f} \right)^{-1} \text{Rd} \right) \frac{\partial^2 \theta}{\partial Y^2} + \left(\frac{\partial^2 \theta}{\partial X^2} \right) = -\frac{\partial \theta}{\partial Y} \frac{\partial \Psi}{\partial X} + \frac{\partial \Psi}{\partial Y} \frac{\partial \theta}{\partial X} \end{aligned} \tag{9}$$

with following new parameters:

$$\begin{aligned} \text{Pr} &= \nu_f / \alpha_f, \text{Ra} = g(\rho\beta)_f \Delta T L^3 / (\mu_f \alpha_f), \text{Ha} = \text{LB}_0 \sqrt{\sigma_f / \mu_f} \\ A_1 &= \frac{\rho_{nf}}{\rho_f}, A_2 = \frac{(\rho C_p)_{nf}}{(\rho C_p)_f}, A_3 = \frac{(\rho\beta)_{nf}}{(\rho\beta)_f}, \\ A_4 &= \frac{k_{nf}}{k_f}, A_5 = \frac{\mu_{nf}}{\mu_f}, A_6 = \frac{\sigma_{nf}}{\sigma_f} \end{aligned} \tag{10}$$

Finally, the rate of heat transfer was estimated using Eq. (11) expressed below:

$$\text{Nu}_{ave} = \frac{1}{S} \int_0^s \text{Nu}_{loc} ds, \quad \text{Nu}_{loc} = \left(\frac{4}{3} (A_4)^{-1} \text{Rd} + 1 \right) \frac{\partial \theta}{\partial n} \left(\frac{k_{nf}}{k_f} \right) \tag{11}$$

Results and discussion

Inclusion of hybrid powders into H₂O creates new carrier fluid, and we utilized such material in porous region and insert the magnetic field. CVFEM in-house code was utilized to simulate this article, and influences of active factors were scrutinized. Profile of θ was compared with previous work and is presented in Fig. 2 which indicates that code has nice accuracy. In Table 1, one example of grid analysis was illustrated [129]. This step is the most important step of numerical modeling to gain independent outputs.

Patten of Ψ with rise of Da is shown in Fig. 3. Configurations of θ and Ψ with rise of Ha are depicted in Figs. 4 and 5. Existing two walls with different temperatures lead to form one vortex. Adding external force shifts the vortex center to left side. Permeability and Lorentz effects are opposed to each other. As expected, lower ∇T with rise of Ha changes the

Fig. 2 Verification of CVFEM code (compared with [129])

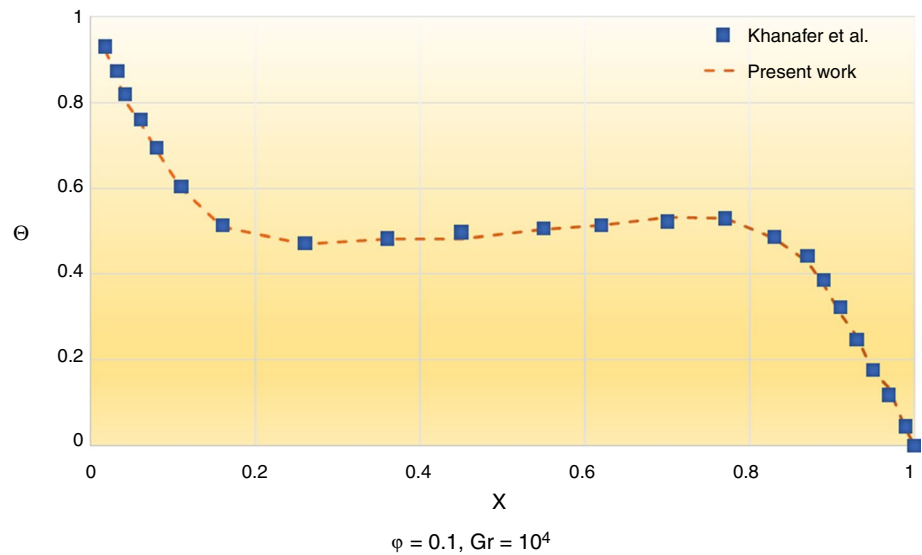


Table 1 Variation of Nu_{ave} with change of mesh size at $Ra = 10^5$, $Rd = 0.8$, $Da = 100$, $Ha = 60$ and $\phi = 0.003$

51×151	61×181	71×211	81×241	91×271
2.5474	2.5474	2.5474	2.5474	2.5474

main mechanism and provides weaker vortex. With insertion of magnetic force, opposed flow changes the modes from convection to conduction and such behavior can be seen from isotherms changes. Distortion of isotherms increases for greater buoyancy effect, but it changes in appearance of magnetic field. Although increasing Da and Ra generates the thermal plume, adding magnetic field makes it to disappear which is attributed with lower convective strength. Undesirable impact of Ha on Nu_{ave} is relevant to this fact that Lorentz forces make nanomaterial flow to reduce. Influence of Da at high Hartmann

number is insignificant. To exhibit the various values of Nu_{ave} , Fig. 6 was demonstrated which is based on below equation:

$$\begin{aligned}
 Nu_{ave} = & 1.48 + 0.038Da^* \log(Ra) \\
 & - 0.17 Ha^* Rd + 0.85 \log(Ra) \\
 & + 0.023Da^* - 0.16Ha^* - 0.015Da^* Ha^* \\
 & + 0.021Rd Da^* + 0.81Rd - 0.32Ha^* \log(Ra)
 \end{aligned} \tag{12}$$

Augmentation of Da which is related to augmentation in permeability makes Nu_{ave} to increase, while Ha has reverse relationship. Both Ra and Rd can enhance the Nu_{ave} , so ∇T augments with rise of them. Transverse flow can be achieved with rise of Ha which suppresses the nanomaterial flow and reduces the ∇T . Negative effect on Nu_{ave} is reported with rise of Ha . Greater values of Rd provide more negative effect of

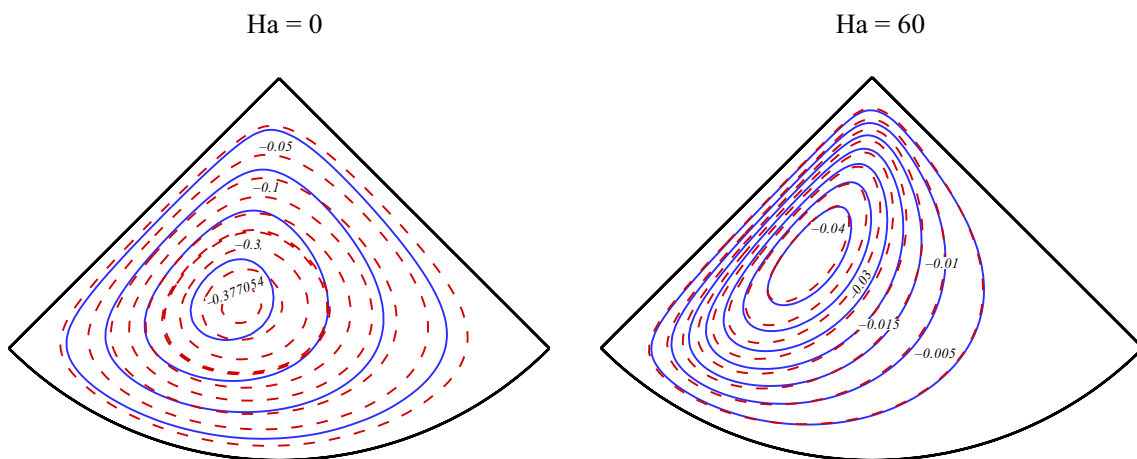


Fig. 3 Patten of Ψ with rise of Da ($Da = 100$ (—) and $Da = 0.01$ (---)) when $Ra = 10^3$, $Rd = 0.8$

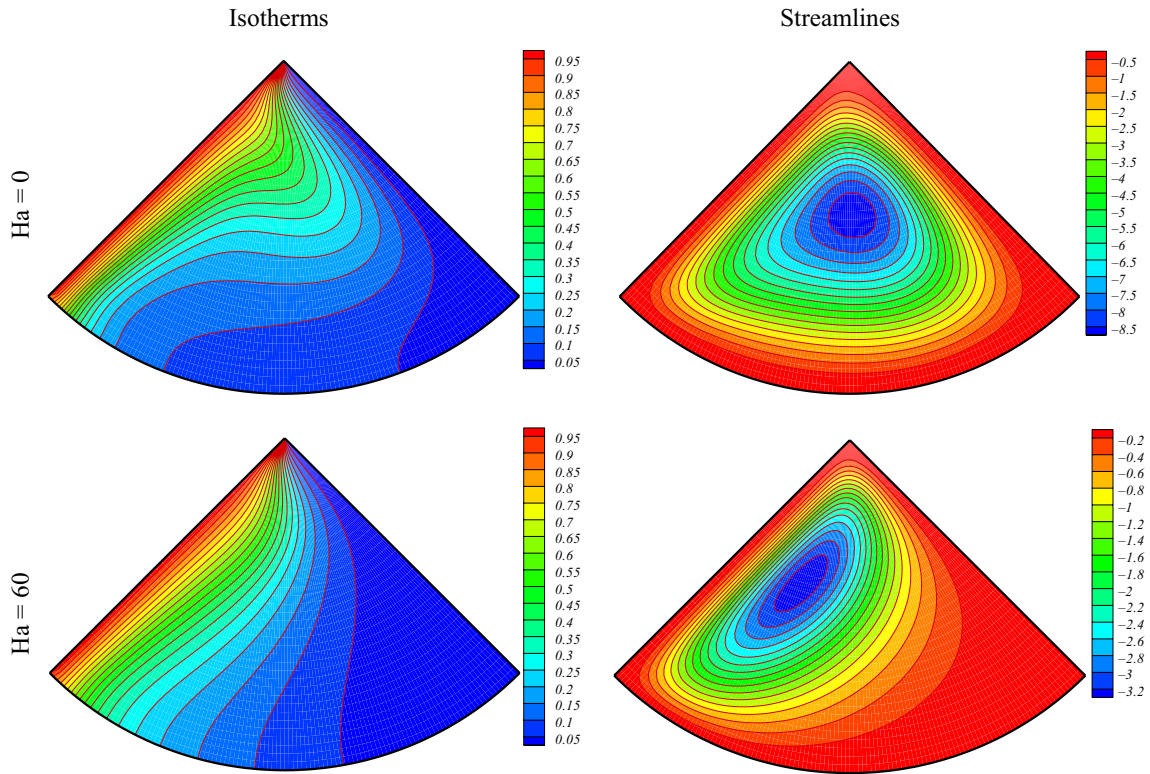


Fig. 4 Configuration of θ and Ψ with rise of Ha at $Ra = 10^5, Da = 0.01, Rd = 0.8$

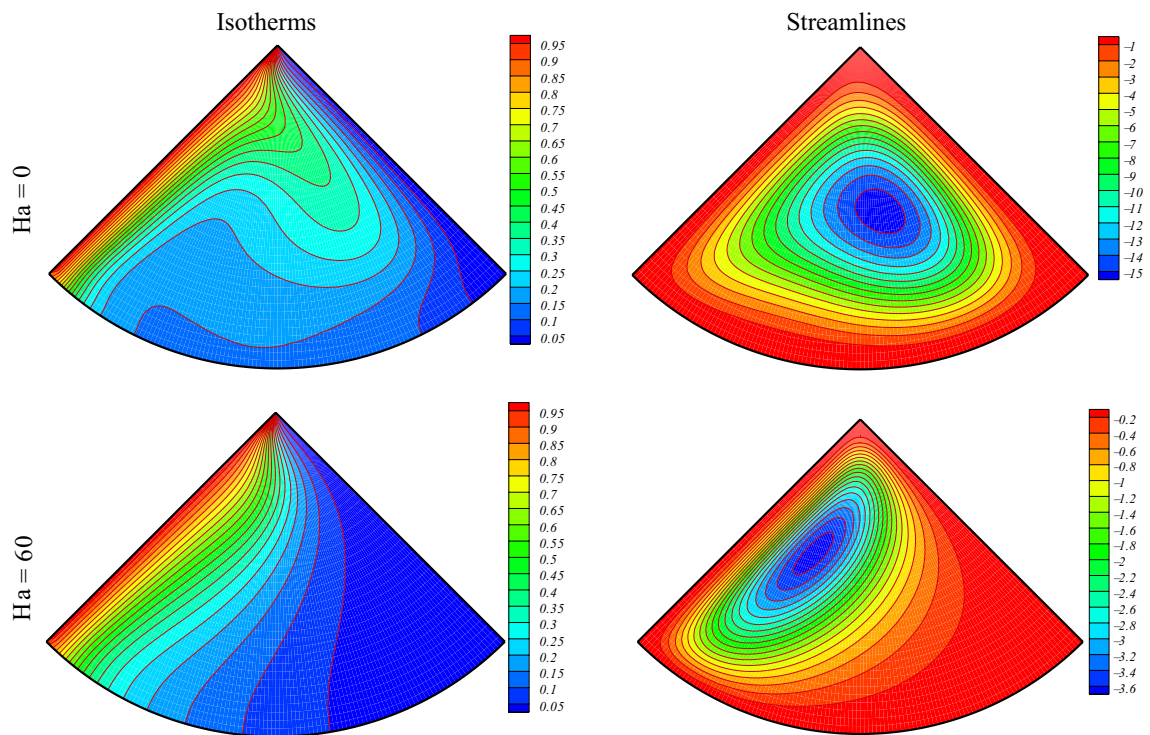


Fig. 5 Configuration of θ and Ψ with rise of Ha at $Ra = 10^5, Da = 100, Rd = 0.8$

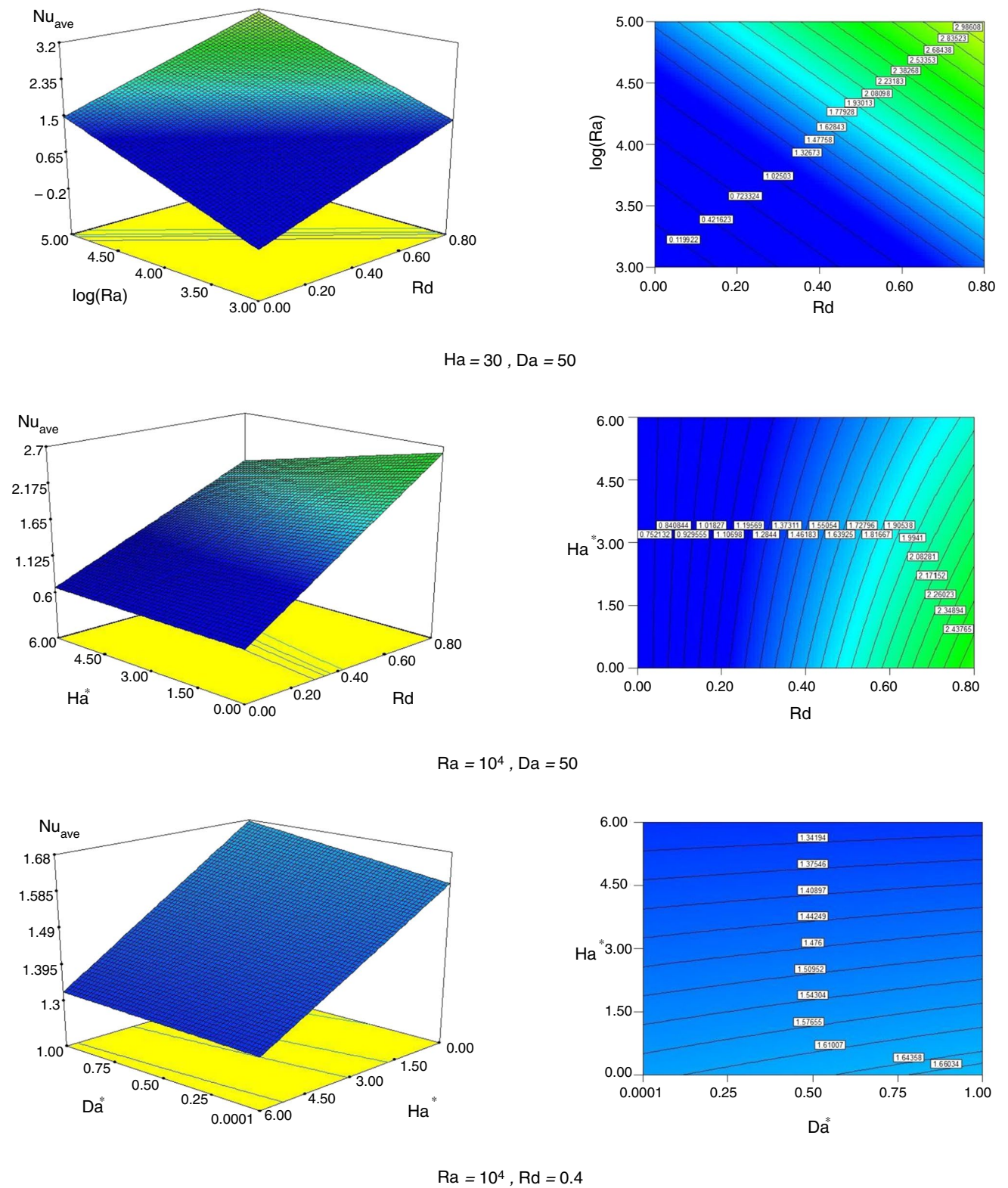


Fig. 6 Nu_{ave} versus active parameters

Ha. Besides, as R_d augments Nu_{ave} can enhance according to definition of this factor.

Conclusions

An application of new in-house code for simulating nanomaterial flow has been presented. To manage the treatment of hybrid powders, Lorentz force was applied. Outcomes are classified to exhibit the effect of scrutinized factors. With respect to lower temperature gradient, Nu_{ave} decreases with augment of Ha, but reverse trend is reported for Da. With rise of permeability, better mixing of nanomaterial is occurred which provides stronger convective flow. Appearance of magnetic force has unfavorable impact of ∇T , and such impact will maximize with increase in R_d .

Acknowledgements Dr. Abdul Khader Jilani would like to thank Dean-ship of Scientific Research at Majmaah University for supporting this paper under the Project Number No. R-1441-11.

References

1. Sheikholeslami M, Arabkoohsar A. Houman Babazadeh, modeling of nanomaterial treatment through a porous space including magnetic forces. *J Therm Anal Calorim.* 2019. <https://doi.org/10.1007/s10973-019-08878-2>.
2. Sheikholeslami M, Barzegar Gerdroodbary M, Shafee A, Tlili I. Hybrid nanoparticles dispersion into water inside a porous wavy tank involving magnetic force. *J Therm Anal Calorim.* 2019. <https://doi.org/10.1007/s10973-019-08858-6>.
3. Qin Y, He H, Ou X, Bao T. Experimental study on darkening water-rich mud tailings for accelerating desiccation. *J Clean Prod.* 2019. <https://doi.org/10.1016/j.jclepro.2019.118235>.
4. Sheikholeslami M, Arabkoohsar A, Jafaryar M. Impact of a helical-twisting device on nanofluid thermal hydraulic performance of a tube. *J Therm Anal Calorim.* 2019. <https://doi.org/10.1007/s10973-019-08683-x>.
5. Seyednezhad M, Sheikholeslami M, Ali JA, Shafee A, Khang Nguyen T. Nanoparticles for water desalination in solar heat exchanger: review. *J Therm Anal Calorim.* 2019. <https://doi.org/10.1007/s10973-019-08634-6>.
6. Sheikholeslami M, Sheremet MA, Shafee A, Li Z. CVFEM approach for EHD flow of nanofluid through porous medium within a wavy chamber under the impacts of radiation and moving walls. *J Therm Anal Calorim.* 2019. <https://doi.org/10.1007/s10973-019-08235-3>.
7. Farshad SA, Sheikholeslami M. Simulation of exergy loss of nanomaterial through a solar heat exchanger with insertion of multi-channel twisted tape. *J Therm Anal Calorim.* 2019. <https://doi.org/10.1007/s10973-019-08156-1>.
8. Sheikholeslami M, Jafaryar M, Shafee A, Li Z. Nanofluid heat transfer and entropy generation through a heat exchanger considering a new turbulator and CuO nanoparticles. *J Therm Anal Calorim.* 2019. <https://doi.org/10.1007/s10973-018-7866-7>.
9. Qin Y, Hiller JE, Meng D. Linearity between pavement thermo-physical properties and surface temperatures. *J Mater Civ Eng.* 2019. [https://doi.org/10.1061/\(ASCE\)MT.1943-5533.0002890](https://doi.org/10.1061/(ASCE)MT.1943-5533.0002890).
10. Vo DD, Hedayat M, Ambreen T, Shehzad SA, Sheikholeslami M, Shafee A, Nguyen TK. Effectiveness of various shapes of Al₂O₃ nanoparticles on the MHD convective heat transportation in porous medium: CVFEM modeling. *J Therm Anal Calorim.* 2019. <https://doi.org/10.1007/s10973-019-08501-4>.
11. Nguyen TK, Sheikholeslami M, Jafaryar M, Shafee A, Li Z, Chandra Mouli KVV, Tlili I. Design of heat exchanger with combined turbulator. *J Therm Anal Calorim.* 2019. <https://doi.org/10.1007/s10973-019-08401-7>.
12. Li Z, Sheikholeslami M, Jafaryar M, Shafee A. Time dependent heat transfer simulation for NEPCM solidification inside a channel. *J Therm Anal Calorim.* 2019. <https://doi.org/10.1007/s10973-019-08140-9>.
13. Qin Y, Luo J, Chen Z, Mei G, Yan L-E. Measuring the albedo of limited-extent targets without the aid of known-albedo masks. *Sol Energy.* 2018;171:971–6.
14. Qin Y. A review on the development of cool pavements to mitigate urban heat island effect. *Renew Sustain Energy Rev.* 2015;52:445–59.
15. Sheikholeslami M. Magnetic source impact on nanofluid heat transfer using CVFEM. *Neural Comput Appl.* 2018;30(4):1055–64.
16. Sheikholeslami M. Application of Darcy law for nanofluid flow in a porous cavity under the impact of Lorentz forces. *J Mol Liq.* 2018;266:495–503.
17. Sheikholeslami M, Arabkoohsar A, Khan I, Shafee A, Li Z. Impact of Lorentz forces on Fe₃O₄-water ferrofluid entropy and exergy treatment within a permeable semi annulus. *J Clean Prod.* 2019;221:885–98.
18. Sheikholeslami M, Rezaeianjouybari B, Darzi M, Shafee A, Li Z, Nguyen TK. Application of nano-refrigerant for boiling heat transfer enhancement employing an experimental study. *Int J Heat Mass Transf.* 2019;141:974–80.
19. Alkanhal TA, Sheikholeslami M, Usman M, Rizwan-ul Haq, Shafee A, Al-Ahmadi AS, Tlili I. Thermal management of MHD nanofluid within the porous medium enclosed in a wavy shaped cavity with square obstacle in the presence of radiation heat source. *Int J Heat Mass Transf.* 2019;139:87–94.
20. Sheikholeslami M, Jafaryar M, Hedayat M, Shafee A, Li Z, Nguyen TK, Bakouri M. Heat transfer and turbulent simulation of nanomaterial due to compound turbulator including irreversibility analysis. *Int J Heat Mass Transf.* 2019;137:1290–300.
21. Qin Y, He Y, Hiller JE, Mei G. A new water-retaining paver block for reducing runoff and cooling pavement. *J Clean Prod.* 2018;199:948–56.
22. Qin Y, Zhao Y, Chen X, Wang L, Li F, Bao T. Moist curing increases the solar reflectance of concrete. *Constr Build Mater.* 2019;215:114–8.
23. Sheikholeslami M, Sajjadi H, Delouei AA, Atashafrooz M, Li Z. Magnetic force and radiation influences on nanofluid transportation through a permeable media considering Al₂O₃ nanoparticles. *J Therm Anal Calorim.* 2019. <https://doi.org/10.1007/s10973-018-7901-8>.
24. Jafaryar M, Sheikholeslami M, Li Z, Moradi R. Nanofluid turbulent flow in a pipe under the effect of twisted tape with alternate axis. *J Therm Anal Calorim.* 2019;135(1):305–23. <https://doi.org/10.1007/s10973-018-7093-2>.
25. Trang TNQ, Tu LTN, Man TV, Mathesh M, Thu VTH, Nam ND. A high-efficiency photoelectrochemistry of Cu₂O/TiO₂ nanotubes for hydrogen evolution under sunlight. *Compos B Eng.* 2019;174:106969.
26. Sheikholeslami M, Jafaryar M, Shafee A, Li Z. Hydrothermal and second law behavior for charging of NEPCM in a two dimensional thermal storage unit. *Chin J Phys.* 2019;58:244–52.
27. Sheikholeslami M, Jafaryar M, Shafee A, Li Z. Simulation of nanoparticles application for expediting melting of PCM inside a finned enclosure. *Physica A.* 2019;523:544–56.

28. Vu NSH, Hien PV, Mathesh M, Thu VTH, Nam ND. Titania nanoparticles impregnated with complex organic molecules' adsorption on steel surface in ethanol fuel blend. *ACS Omega*. 2019;4:146–58.
29. Sheikholeslami M, Gerdroodbary MB, Moradi R, Shafee A, Li Z. Application of neural network for estimation of heat transfer treatment of $\text{Al}_2\text{O}_3\text{-H}_2\text{O}$ nanofluid through a channel. *Comput Methods Appl Mech Eng*. 2019;344:1–12.
30. Sheikholeslami M, Zeeshan A. Analysis of flow and heat transfer in water based nanofluid due to magnetic field in a porous enclosure with constant heat flux using CVFEM. *Comput Methods Appl Mech Eng*. 2017;320:68–81.
31. Sheikholeslami M, Vajravelu K. Nanofluid flow and heat transfer in a cavity with variable magnetic field. *Appl Math Comput*. 2017;298:272–82.
32. Sheikholeslami M, Shamlooei M. $\text{Fe}_3\text{O}_4\text{-H}_2\text{O}$ nanofluid natural convection in presence of thermal radiation. *Int J Hydrogen Energy*. 2017;42(9):5708–18.
33. Sheikholeslami M, Rokni HB. Magnetic nanofluid flow and convective heat transfer in a porous cavity considering Brownian motion effects. *Phys Fluids*. 2018. <https://doi.org/10.1063/1.5012517>.
34. Sheikholeslami M, Rokni HB. Influence of EFD viscosity on nanofluid forced convection in a cavity with sinusoidal wall. *J Mol Liq*. 2017;232:390–5.
35. Sheikholeslami M, Sadoughi MK. Simulation of CuO -water nanofluid heat transfer enhancement in presence of melting surface. *Int J Heat Mass Transf*. 2018;116:909–19.
36. Sheikholeslami M, Rokni HB. Simulation of nanofluid heat transfer in presence of magnetic field: a review. *Int J Heat Mass Transf*. 2017;115:1203–33.
37. Sheikholeslami M, Hayat T, Alsaedi A. On simulation of nanofluid radiation and natural convection in an enclosure with elliptical cylinders. *Int J Heat Mass Transf*. 2017;115:981–91.
38. Sheikholeslami M, Shehzad SA. CVFEM for influence of external magnetic source on $\text{Fe}_3\text{O}_4\text{-H}_2\text{O}$ nanofluid behavior in a permeable cavity considering shape effect. *Int J Heat Mass Transf*. 2017;115:180–91.
39. Sheikholeslami M, Seyednezhad M. Nanofluid heat transfer in a permeable enclosure in presence of variable magnetic field by means of CVFEM. *Int J Heat Mass Transf*. 2017;114:1169–80.
40. Sheikholeslami M, Rokni HB. Melting heat transfer influence on nanofluid flow inside a cavity in existence of magnetic field. *Int J Heat Mass Transf*. 2017;114:517–26.
41. Koblinski P, Phillpot SR, Choi SUS, Eastman JA. Mechanisms of heat flow in suspensions of nano-sized particles (nanofluids). *Int J Heat Mass Transf*. 2002;45:855–63.
42. Javed T, Siddiqui MA. Effect of MHD on heat transfer through ferrofluid inside a square cavity containing obstacle/heat source. *Int J ThermSci*. 2018;125:419–27.
43. Muthamilselvan M, Periyadurai K, Doh DH. Effect of uniform and nonuniform heat source on natural convection flow of micropolar fluid. *Int J Heat Mass Transf*. 2017;115:19–34.
44. Sheikholeslami M. Investigation of coulomb forces effects on ethylene glycol based nanofluid laminar flow in a porous enclosure. *Appl Math Mech (Engl Ed)*. 2018;39(9):1341–52.
45. Sheikholeslami M. Numerical simulation for solidification in a LHTESS by means of nano-enhanced PCM. *J Taiwan Inst Chem Eng*. 2018;86:25–41.
46. Sheikholeslami M. Numerical modeling of nano enhanced PCM solidification in an enclosure with metallic fin. *J Mol Liq*. 2018;259:424–38.
47. Qin Y, Zhang M, Hiller JE. Theoretical and experimental studies on the daily accumulative heat gain from cool roofs. *Energy*. 2017;129:138–47.
48. Sheikholeslami M, Rokni HB. Nanofluid two phase model analysis in existence of induced magnetic field. *Int J Heat Mass Transf*. 2017;107:288–99.
49. Sheikholeslami M, Hayat T, Alsaedi A, Abelman S. Numerical analysis of EHD nanofluid force convective heat transfer considering electric field dependent viscosity. *Int J Heat Mass Transf*. 2017;108:2558–65.
50. Sheikholeslami M, Shehzad SA. Magnetohydrodynamic nanofluid convection in a porous enclosure considering heat flux boundary condition. *Int J Heat Mass Transf*. 2017;106:1261–9.
51. Qin Y, He H. A new simplified method for measuring the albedo of limited extent targets. *Solar Energy*. 2017;157(Supplement C):1047–55.
52. Qin Y, He Y, Wu B, Ma S, Zhang X. Regulating top albedo and bottom emissivity of concrete roof tiles for reducing building heat gains. *Energy Build*. 2017;156(Supplement C):218–24.
53. Qin Y. Pavement surface maximum temperature increases linearly with solar absorption and reciprocal thermal inertial. *Int J Heat Mass Transf*. 2016;97:391–9.
54. Sheikholeslami M, Shehzad SA. Thermal radiation of ferrofluid in existence of Lorentz forces considering variable viscosity. *Int J Heat Mass Transf*. 2017;109:82–92.
55. Sheikholeslami M, Hayat T, Alsaedi A. Numerical study for external magnetic source influence on water based nanofluid convective heat transfer. *Int J Heat Mass Transf*. 2017;106:745–55.
56. Sheikholeslami M, Hayat T, Alsaedi A. MHD free convection of $\text{Al}_2\text{O}_3\text{-water}$ nanofluid considering thermal radiation: a numerical study. *Int J Heat Mass Transf*. 2016;96:513–24.
57. Sheikholeslami M, Ellahi R. Three dimensional mesoscopic simulation of magnetic field effect on natural convection of nanofluid. *Int J Heat Mass Transf*. 2015;89:799–808.
58. Wang R, Sheikholeslami M, Mahmood BS, Shafee A, Nguyen-Thoi T. Simulation of triplex-tube heat storage including nanoparticles, solidification process. *J Mol Liq*. 2019. <https://doi.org/10.1016/j.molliq.2019.111731>.
59. Sheikholeslami M. Effect of uniform suction on nanofluid flow and heat transfer over a cylinder. *J Braz Soc Mech Sci Eng*. 2015;37:1623–33.
60. Ma X, Sheikholeslami M, Jafaryar M, Shafee A, Nguyen-Thoi T, Li Z. Solidification inside a clean energy storage unit utilizing phase change material with copper oxide nanoparticles. *J Clean Prod*. 2019. <https://doi.org/10.1016/j.jclepro.2019.118888>.
61. Sheikholeslami M, Mahian O. Enhancement of PCM solidification using inorganic nanoparticles and an external magnetic field with application in energy storage systems. *J Clean Prod*. 2019;215:963–77.
62. Qin Y, Liang J, Tan K, Li F. A side by side comparison of the cooling effect of building blocks with retro-reflective and diffuse-reflective walls. *Sol Energy*. 2016;133:172–9.
63. Qin Y, Liang J, Yang H, Deng Z. Gas permeability of pervious concrete and its implications on the application of pervious pavements. *Measurement*. 2016;78:104–10.
64. Nguyen TK, Usman M, Sheikholeslami M, Rizwan-ul Haq, Shafee A, Jilani AK, Tlili I. Numerical analysis of MHD flow and nanoparticle migration within a permeable space containing non-equilibrium model. *Physica A: Stat Mech Appl*. 2020;537:122459.
65. Sheikholeslami M, Jafaryar M, Ali JA, Hamad SM, Divsalar A, Shafee A, Nguyen-Thoi T, Li Z. Simulation of turbulent flow of nanofluid due to existence of new effective turbulator involving entropy generation. *J Mol Liq*. 2019;291:111283.
66. Qin Y, Hiller JE. Understanding pavement-surface energy balance and its implications on cool pavement development. *Energy Build*. 2014;85:389–99.

67. Qin Y, Zhang M, Mei G. A new simplified method for measuring the permeability characteristics of highly porous media. *J Hydrol.* 2018;562:725–32.
68. Sheikholeslami M. Magnetic field influence on nanofluid thermal radiation in a cavity with tilted elliptic inner cylinder. *J Mol Liq.* 2017;229:137–47.
69. Sheikholeslami M. Numerical simulation of magnetic nanofluid natural convection in porous media. *Phys Lett A.* 2017;381:494–503.
70. Sheikholeslami M. Influence of Lorentz forces on nanofluid flow in a porous cylinder considering Darcy model. *J Mol Liq.* 2017;225:903–12.
71. Sheikholeslami M. CVFEM for magnetic nanofluid convective heat transfer in a porous curved enclosure. *Eur Phys J Plus.* 2016;131:413. <https://doi.org/10.1140/epjp/i2016-16413-y>.
72. Sheikholeslami M. Influence of Coulomb forces on Fe₃O₄-H₂O nanofluid thermal improvement. *Int J Hydrogen Energy.* 2017;42:821–9.
73. Saravanan S, Sivaraj C. Combined natural convection and thermal radiation in a square cavity with a nonuniformly heated plate. *Comput Fluids.* 2015;117:125–38.
74. Gangawane KM, Oztop HF, Abu-Hamdeh N. Mixed convection characteristic in a lid-driven cavity containing heated triangular block: effect of location and size of block. *Int J Heat Mass Transf.* 2018;124:860–75.
75. Mehmood K, Hussain S, Sagheer M. Mixed convection in alumina-water nanofluid filled lid-driven square cavity with an isothermally heated square blockage inside with magnetic field effect: introduction. *Int J Heat Mass Transf.* 2017;109:397–409.
76. Eastman JA, Choi SUS, Li S, Yu W, Thompson LJ. Anomalous increased effective thermal conductivities of ethylene glycol-based nanofluids containing copper nanoparticles. *Appl Phys Lett.* 2001;78:718–20.
77. Zhang X, Liu W. New criterion for local thermal equilibrium in porous media. *J Thermophys Heat Transf.* 2008;22:649–53.
78. Kalidasan K, Velkennedy R, Kanna PR. Natural convection heat transfer enhancement using nanofluid and time-variant temperature on the square enclosure with diagonally constructed twin adiabatic blocks. *Appl Therm Eng.* 2016;92:219–35.
79. Mahalakshmi T, Nithyadevi N, Oztop HF, Abu-Hamdeh N. Natural convective heat transfer of Ag–water nanofluid flow inside enclosure with center heater and bottom heat source. *Chin J Phys.* 2018;56:1497–507.
80. Sheikholeslami M. Finite element method for PCM solidification in existence of CuO nanoparticles. *J Mol Liq.* 2018;265:347–55.
81. Qin Y. Urban canyon albedo and its implication on the use of reflective cool pavements. *Energy Build.* 2015;96:86–94.
82. Sheikholeslami M. New computational approach for exergy and entropy analysis of nanofluid under the impact of Lorentz force through a porous media. *Comput Methods Appl Mech Eng.* 2019;344:319–33.
83. Sheikholeslami M. Numerical approach for MHD Al₂O₃–water nanofluid transportation inside a permeable medium using innovative computer method. *Comput Methods Appl Mech Eng.* 2019;344:306–18.
84. Sheikholeslami M. Solidification of NEPCM under the effect of magnetic field in a porous thermal energy storage enclosure using CuO nanoparticles. *J Mol Liq.* 2018;263:303–15.
85. Sheikholeslami M. Influence of magnetic field on Al₂O₃-H₂O nanofluid forced convection heat transfer in a porous lid driven cavity with hot sphere obstacle by means of LBM. *J Mol Liq.* 2018;263:472–88.
86. Sheikholeslami M. Numerical investigation of nanofluid free convection under the influence of electric field in a porous enclosure. *J Mol Liq.* 2018;249:1212–21.
87. Sheikholeslami M. CuO–water nanofluid flow due to magnetic field inside a porous media considering Brownian motion. *J Mol Liq.* 2018;249:921–9.
88. Sheikholeslami M. Numerical investigation for CuO–H₂O nanofluid flow in a porous channel with magnetic field using mesoscopic method. *J Mol Liq.* 2018;249:739–46.
89. Sheikholeslami M. Numerical simulation for external magnetic field influence on Fe₃O₄–water nanofluid forced convection. *Eng Comput.* 2018;35(4):1639–54. <https://doi.org/10.1108/EC-06-2017-0200>.
90. Sheikholeslami M. Magnetic field influence on CuO–H₂O nanofluid convective flow in a permeable cavity considering various shapes for nanoparticles. *Int J Hydrogen Energy.* 2017;42:19611–21.
91. Sheikholeslami M. Influence of Lorentz forces on nanofluid flow in a porous cavity by means of non-Darcy model. *Eng Comput.* 2017;34(8):2651–67. <https://doi.org/10.1108/EC-01-2017-0008>.
92. Sheikholeslami M. Lattice Boltzmann method simulation of MHD non-Darcy nanofluid free convection. *Phys B.* 2017;516:55–71.
93. Sheikholeslami M. Influence of magnetic field on nanofluid free convection in an open porous cavity by means of lattice Boltzmann method. *J Mol Liq.* 2017;234:364–74.
94. Sheikholeslami M. Magnetohydrodynamic nanofluid forced convection in a porous lid driven cubic cavity using lattice Boltzmann method. *J Mol Liq.* 2017;231:555–65.
95. Sheikholeslami M. CuO–water nanofluid free convection in a porous cavity considering Darcy law. *Eur Phys J Plus.* 2017;132:55. <https://doi.org/10.1140/epjp/i2017-11330-3>.
96. Sheikholeslami M. Numerical investigation of MHD nanofluid free convective heat transfer in a porous tilted enclosure. *Eng Comput.* 2017;34(6):1939–55.
97. Sheikholeslami M, Jafaryar M, Shafee A, Li Z, Rizwan. Heat transfer of nanoparticles employing innovative turbulator considering entropy generation. *Int J Heat Mass Transf.* 2019;136:1233–40.
98. Sheikholeslami M, Rizwan-ul Haq, Shafee A, Li Z, Elaraki YG, Tili I. Heat transfer simulation of heat storage unit with nanoparticles and fins through a heat exchanger. *Int J Heat Mass Transf.* 2019;135:470–8.
99. Sheikholeslami M, Rizwan-ul Haq, Shafee A, Li Z. Heat transfer behavior of Nanoparticle enhanced PCM solidification through an enclosure with V shaped fins. *Int J Heat Mass Transf.* 2019;130:1322–42.
100. Sheikholeslami M, Shehzad SA, Li Z, Shafee A. Numerical modeling for Alumina nanofluid magnetohydrodynamic convective heat transfer in a permeable medium using Darcy law. *Int J Heat Mass Transf.* 2018;127:614–22.
101. Soomro FA, Zaib A, Haq RU, Sheikholeslami M. Dual nature solution of water functionalized copper nanoparticles along a permeable shrinking cylinder: FDM approach. *Int J Heat Mass Transf.* 2019;129:1242–9.
102. Sheikholeslami M, Li Z, Shafee A. Lorentz forces effect on NEPCM heat transfer during solidification in a porous energy storage system. *Int J Heat Mass Transf.* 2018;127:665–74.
103. Sheikholeslami M, Jafaryar M, Saleem S, Li Z, Shafee A, Jiang Y. Nanofluid heat transfer augmentation and exergy loss inside a pipe equipped with innovative turbulators. *Int J Heat Mass Transf.* 2018;126:156–63.
104. Sheikholeslami M, Ghasemi A, Li Z, Shafee A, Saleem S. Influence of CuO nanoparticles on heat transfer behavior of PCM in solidification process considering radiative source term. *Int J Heat Mass Transf.* 2018;126:1252–64.
105. Sheikholeslami M, Darzi M, Li Z. Experimental investigation for entropy generation and exergy loss of nano-refrigerant condensation process. *Int J Heat Mass Transf.* 2018;125:1087–95.

106. Sheikholeslami M, Shehzad SA, Li Z. Water based nanofluid free convection heat transfer in a three dimensional porous cavity with hot sphere obstacle in existence of Lorenz forces. *Int J Heat Mass Transf.* 2018;125:375–86.
107. Sheikholeslami M, Jafaryar M, Li Z. Nanofluid turbulent convective flow in a circular duct with helical turbulators considering CuO nanoparticles. *Int J Heat Mass Transf.* 2018;124:980–9.
108. Sheikholeslami M, Ghasemi A. Solidification heat transfer of nanofluid in existence of thermal radiation by means of FEM. *Int J Heat Mass Transf.* 2018;123:418–31.
109. Sheikholeslami M, Shehzad SA. CVFEM simulation for nanofluid migration in a porous medium using Darcy model. *Int J Heat Mass Transf.* 2018;122:1264–71.
110. Sheikholeslami M, Darzi M, Sadoughi MK. Heat transfer improvement and Pressure Drop during condensation of refrigerant-based nanofluid: an experimental procedure. *Int J Heat Mass Transf.* 2018;122:643–50.
111. Sheikholeslami M, Shehzad SA. Simulation of water based nanofluid convective flow inside a porous enclosure via non-equilibrium model. *Int J Heat Mass Transf.* 2018;120:1200–12.
112. Sheikholeslami M, Seyednezhad M. Simulation of nanofluid flow and natural convection in a porous media under the influence of electric field using CVFEM. *Int J Heat Mass Transf.* 2018;120:772–81.
113. Sheikholeslami M, Rokni HB. Numerical simulation for impact of Coulomb force on nanofluid heat transfer in a porous enclosure in presence of thermal radiation. *Int J Heat Mass Transf.* 2018;118:823–31.
114. Sheikholeslami M, Shehzad SA. Numerical analysis of Fe_3O_4 – H_2O nanofluid flow in permeable media under the effect of external magnetic source. *Int J Heat Mass Transf.* 2018;118:182–92.
115. Nguyen DT, Dang LH, Dinh VT, Nam ND, Giang BL, Nguyen CT, Thanh VM, Thu LV, Tran QN. Dual interactions of amphiphilic gelatin copolymer and nanocurcumin enhancing the loading efficiency of the nanogels. *Polymers.* 2019;11:814. <https://doi.org/10.3390/polym11050814>.
116. Sheikholeslami M, Sadoughi M. Mesoscopic method for MHD nanofluid flow inside a porous cavity considering various shapes of nanoparticles. *Int J Heat Mass Transf.* 2017;113:106–14.
117. Sheikholeslami M, Bhatti MM. Forced convection of nanofluid in presence of constant magnetic field considering shape effects of nanoparticles. *Int J Heat Mass Transf.* 2017;111:1039–49.
118. Sheikholeslami M, Bhatti MM. Active method for nanofluid heat transfer enhancement by means of EHD. *Int J Heat Mass Transf.* 2017;109:115–22.
119. Hedayat M, Sheikholeslami M, Shafee A, Nguyen-Thoi T, Ben Henda M, Tlili I, Li Z. Investigation of nanofluid conduction heat transfer within a triplex tube considering solidification. *J Mol Liq.* 2019;290:111232.
120. Farshad SA, Sheikholeslami M. FVM modeling of nanofluid forced convection through a solar unit involving MCTT. *Int J Mech Sci.* 2019;159:126–39.
121. Farshad SA, Sheikholeslami M. Nanofluid flow inside a solar collector utilizing twisted tape considering exergy and entropy analysis. *Renew Energy.* 2019;141:246–58.
122. Nam ND. Improvement of mechanical properties and saline corrosion resistance of extruded Mg–8Gd–4Y–0.5Zr by alloying with 2 wt% Zn. *J Alloys Compd.* 2017;412:464–74.
123. Sheikholeslami M, Zareei A, Jafaryar M, Shafee A, Li Z, Smida A, Tlili I. Heat transfer simulation during charging of nanoparticle enhanced PCM within a channel. *Physica A: Stat Mech Appl.* 2019;525:557–65.
124. Le TNT, Ton NQT, Tran VM, Nam ND, Vu THT. TiO₂ nanotubes with different Ag loading to enhance visible-light photocatalytic activity. *J Nanomater.* 2017;2017:1–7.
125. Sivaraj C, Sheremet MA. MHD natural convection in an inclined square porous cavity with a heat conducting solid block. *J MagnMagn Mater.* 2017;426:351–60.
126. Yu W, Choi SUS. The role of interfacial layer in the enhanced thermal conductivity. ofnanofluids: a renovated Maxwell model. *J Nanoparticle Res.* 2003;5:167–71.
127. Sheikholeslami M, Mehryan SAM, Shafee A, Mikhail A. Variable magnetic forces impact on magnetizable hybrid nanofluid heat transfer through a circular cavity. *J Mol Liq.* 2019;277:388–96.
128. Sheikholeslami M. Application of control volume based finite element method (CVFEM) for nanofluid flow and heat transfer. Elsevier; (2019), ISBN: 9780128141526.
129. Khanafer K, Vafai K, Lightstone M. Buoyancy-driven heat transfer enhancement in a two-dimensional enclosure utilizing nanofluids. *Int J Heat Mass Transf.* 2003;46:3639–53.

Publisher's Note Springer Nature remains neutral with regard to jurisdictional claims in published maps and institutional affiliations.